Journal of
Mechanical
Science and
Technology

Journal of Mechanical Science and Technology 21 (2007) 1048~1057

# Analysis of the Braking System of the Korean High-Speed Train Using Real-time Simulations

Chul-Goo Kang*

*Department of Mechanical Engineering, Konkuk University, Seoul 143-701, Korea*

(Manuscript Received November 7, 2006; Revised April 18, 2007; Accepted April 18, 2007)

**Abstract**

The braking system of a high-speed train has a crucial role for the safety of human mass transportation. However, it is hard to acquire design parameters of the braking system in the development stage of a new high-speed train. In this paper, we build a Hardware-In-the-Loop (HIL) system for the braking system of the Korean High-Speed Train (KHST) that is supposed to reach 350 km/h, and analyze the characteristics of the braking system of KHST (composed of 7 cars) via real-time simulations. In the HIL system that is built using a DSP board of dSPACE, the dynamics of the 7 car bodies and several bogies and characteristics of connecting devices between cars are considered individually. Simulation results show that the designed braking system of KHST is valid and satisfies design specifications.

*Keywords:* Braking system; High-speed train; Real-time simulation; HILS; Bogie

## 1. Introduction

The Seoul-Busan High-Speed Train, called Korea Train Express (KTX), launched its test runs of 300 km/h in December 1999 via TGV technology under an agreement with TGV of France, and has laid new ground on the landmark development of Korea's railroad technology. Aside from the KTX, the project to develop the Korean version of the high-speed train, so-called Korean High-Speed Train (KHST) is now under way as a government-led corporation (Chung, 1998). The goal of the Korean High-Speed Train project is to develop a high-speed train system capable of reaching a speed of 350 km/h and to secure its key technologies, one of which is the braking technology of high-speed trains.

To enhance speed and secure safety, advanced countries such as Japan, France and Germany have long conducted research on the dynamics and control of the high-speed train (Miyachi et al., 1996; Rahn, 1986), which is now shedding light on the nonlinear dynamic analysis taking into consideration the nonlinearity into the linear model. The nonlinear dynamic analysis is made using two different methods, one of decoding the elements of the nonlinearity of the system by means of linearization, and the other of analyzing the nonlinearity as one of the system's important factors. The nonlinear analysis of an entire car is so complicated that it is generally limited to the wheel model and the bogie model. The linear dynamic analysis is usually carried out by ordinary differential equations under the assumption of a lumped-parameter system.

Recently, Kato et al.(2005) proposed a model of the wheel/rail system to deal with complex phenomena of high-speed vehicles in vertical vibrations and showed the validity of it by simulation study. Matsumoto et al.(2005) proposed a *friction control* method, which utilizes friction modifiers with onboard spraying system, and developed a theoretical model of wheel/rail contact condition and simulated it in the

*Corresponding author. Tel.: +82 2 447 2142, Fax.: +82 2 447 5886
E-mail address: cgkang@konkuk.ac.kr

framework of multi-body dynamics (Schiehlen, 2005). Moreover, for the safety of passengers on the platform, Huh et al.(2004) analyzed wind pressure transients in the tunnel inside a station caused by a passing high-speed train.

As far as Korea is concerned, there have been a few attempts to determine and design the constituents and essential parts of the braking system of the train, but the braking system research is still in an early stage. So, it is necessary that we pay more systematic and active attention to this braking system which has a crucial role for the safety of human mass transportation.

Lee et al.(2002) performed off-line computer simulation tests on the braking system of KHST rather than on the real-time basis. Hwang et al.(2001) succeeded in building up the HIL (Hardware-In-the-Loop) system for two cars of KHST.

In this study, we upgraded and completed Hwang's HIL system (Hwang, 2001) of the braking system to seven cars of KHST. Then, we performed real-time simulations on the prototype cars of KHST for the purpose of taking an even closer look at various kinds of operational possibilities when the braking system would eventually be put on the train.

As for the car modeling, we evaluated dynamic equation by linearizing a multi-body dynamics model, which is good in representing the dynamics of real cars in the lumped-parameter system. Then we determined the state variables and induced state equation. We checked out some phenomena on a real-time basis when the braking system is to be put into effect.

We set up the HIL system using a special DSP (Digital Signal Processing) board manufactured by dSPACE (2001) instead of the mechanical hardware of the braking system, fulfilling the real-time simulations in which the applied parameters were adopted by the specifications of the prototype cars of KHST.

## 2. Composition of the prototype of the Korean High-Speed Train

Eventually KHST will consist of 20 compartments in total, such as of 2 power cars, 4 motor cars and 14 trailer cars. However, in this paper, we consider the first prototype of the Korean High-Speed Train that is composed of seven cars as shown in Fig. 1; one power car and one motor car consecutively in front, three trailer cars in the middle, and one motor car and one power car in rear. Each power car is loaded with two power motor bogies, and each motor car is loaded with one motorized trailer bogie and one articulated trailer bogie. The articulated trailer bogie is shared with the following trailer car. Articulated motor bogies are also installed between trailer cars.

The connecting devices between power car and motor car have different compositions from those between motor car and trailer car as shown in Fig. 2, in which simplified symbols are used for elements.

Two buffers and a coupling hook are placed between power car and motor car. Buffers are at the point of 875 mm from the center of car body and of 650 mm from the top of rail; one on the right side and the other on the left side. The height of the flange is constant, and the length of it is dependent on the interference by relative motions between cars and is calculated according to car length and minimum radius of curvature. The buffer at the side of the motor car has a cover to prevent from separation in the vertical direction during relative motions. The stroke is within 110 mm and no force is loaded in normal operations, but compression force acts in braking stages. When more than 1,100 kN acts accidentally, rivets of buffer case are broken and maximum stroke is sustained (Korea Railroad Research Institute, 2002). The coupling hook transmits traction force of up to 1000 kN between power car and motor car, and has a radius of curvature of 150 mm.

The connecting devices between motor car and trailer car and between trailer cars are bogie pivot, articulation device, damper, secondary suspension between body and bogie, and anti-roll bar.

Bogie pivot placed at the bottom of the supporting ring and at the top of the bogie center transmits traction force and brake force. It allows relative angular motions occurring when the train runs on curved rails. The articulation device that is designed to absorb the impact by the metal/rubber shock absorber is one of the most reliable connecting devices that provide cars with traction

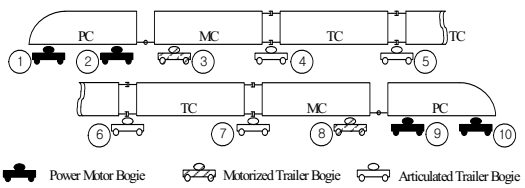


Fig. 1. Formation of the Korean High-Speed Train.

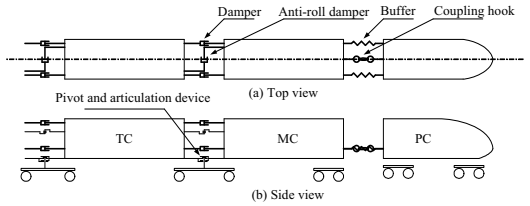


Fig. 2. Connections between cars.

and brake force.

When the train runs on the winding track, the four connecting dampers function as a shock absorber in the longitudinal direction. When car bodies are shaken alternatively from left to right, the anti-heel damper serves as a shock absorber. The damper placed between bogie and car body controls yaw motion and increases stability at high speed.

The air spring, the secondary suspension system, functions as another shock absorber against vertical loads between car body and bogie and allows the bogie to rotate by twisting when the train enters a curve. The air spring consists of auxiliary air cylinder, air bags, auxiliary spring, leveling valve and differential pressure valve. Load of 11 to 14 tons acts on each air spring. Leveling valve enables the height of air spring almost constant (about 48 mm) by adjusting air pressure. The auxiliary spring is a back-up spring for breakdown of air bags, and the differential pressure valve is activated when the pressure difference between right and left air bag exceeds the set point.

The anti-roll bar minimizes rolling motion between bogie frame and car body, and allows restricted rolling motion of car body.

An appropriate braking system is essential to controlling the high-speed train with the proper velocity and acceleration the driver desires. This braking system should be designed with a focus on securing the least attrition of the rail and the wheel, as well as high efficiency. When the braking system is devised, the thermodynamic and dynamic aspects should necessarily be taken into consideration.

From the thermodynamic point of view, the kinetic energy of the train should be transformed into other types of energy with the intention of reducing the speed of the running train. Tread braking, wheel disc braking, and disc braking make use of friction to emit kinetic energy in the shape of heat on the air.

Table 1. Brake units for each bogie.

| Bogie type | No. in Fig. 1 | Brake unit | Numbers |
|---|---|---|---|
| Power motor bogie | 1, 2, 9, 10 | Regenerative brake | 2/bogie |
| | | Reostatic brake | 1/bogie |
| | | Tread brake | 1/wheel |
| Motorized trailer bogie | 3, 8 | Regenerative brake | 2/bogie |
| | | Reostatic brake | 1/bogie |
| | | Wheel disk brake | 1/shaft |
| Articulated trailer bogie | 4,5,6,7 | Eddy-current brake | 1/bogie |
| | | Disk brake | 3/shaft |

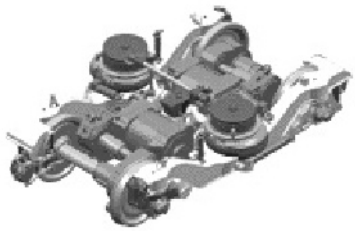

Fig. 3. Motorized trailer bogie for KHST.

Regenerative braking, rheostatic braking, and eddy-current braking transform kinetic energy into electrical energy to recycle or dissipate.

From the dynamics point of view, we should take the following aspects into account; piston pressures used for tread braking, wheel disc braking, and disc braking; brake forces affected by braking efficiency; resistances imposed on the train like air resistance; braking time that it takes the train to come to a complete stop after the brake is applied; braking distance that the train runs during the braking time; and adhesive force that is the maximum friction force between the wheel and the rail. Since adhesive force is in proportion to adhesion coefficient, it is crucial to improve the adhesion coefficient in order to increase maximum brake force.

The adhesive force determines the traction or brake force of the train. When brake torque or traction torque operates beyond the capacity of the adhesive force, the wheel slides and adhesive force instantaneously declines more than when there is no sliding. Therefore, it is important to make sure adhesive force does not exceed the limit to the extent that the wheel and the rail may be damaged.

Refer to the reference (Lee et al., 2002) for the mechanism and figure of each brake unit. Table 1

summarizes brake units used for each bogie. Figure 3 shows the motorized trailer bogie among three types of bogies used for KHST.

## 3. Modeling of the prototype cars of KHST

Figure 4 shows the schematics of the high-speed train's dynamic model we are planning to draw up. Springs and dampers are included for the direction that the train is moving forward (*x* direction) and the vertical direction that the train is moving toward (*y* direction), respectively.

To simplify the model, we did not consider the rolling motion, yawing motion and lateral motion of the train, but consider only the plane motion of the train in the *x*-*y* plane.

The dynamic modeling of KHST has been undertaken as follows: segmenting entire cars, drawing out separate free-body diagrams of the car body, the bogie, and the wheel, inducing the equations of motion, defining state variables, and then deriving state equations.

Figure 5 shows the free-body diagram of the *n*-th car body. In the figure, $F_{fp}[n]$ and $F_{rp}[n]$ are forces acting on the *n*-the car body by the center pivot inserted into the center of the bogie. Here subscript *f* implies front and *r* implied rear. $F_{ar}[n]$ is air resistance acting on the center of gravity of the *n*-th car body. Air resistance is determined from the experimental equation and then is distributed to each car appropriately. $F_{fud}[n]$ and $F_{fld}[n]$ are forces acting on the car body by the dampers connected to (*n*+1)-th car body, and $F_{rud}[n]$ and $F_{rld}[n]$ are forces acting on the car body by the dampers connected to (*n*-1)-th car body, where subscript *u* implies upper and *l* implies lower. $R_{fb}[n]$ and $R_{rb}[n]$ are reaction forces acting vertically by the bogies. $h_{b1}$ through $h_{b5}$ are distances from the center of gravity of the car body to each point where the force acts. $\theta_b$ is the rotating angle in the *x*-*y* plane about the center of gravity.

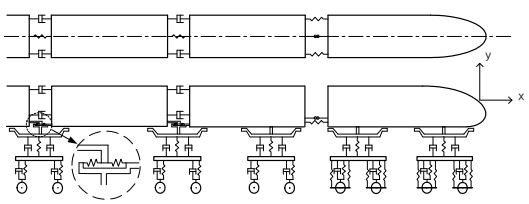


Fig. 4. Schematic model of the train dynamics.

Equations of motion for the *n*-th car body are as follows from the free-body diagram shown in Fig. 5.

$$\begin{aligned} M_b[n]\ \ddot{x}_b &= \left(F_{fud}[n]+F_{fld}[n]\right)-\left(F_{rud}[n]+F_{rld}[n]\right)-F_{ar}[n] \\ &\quad -\left\{F_{break}[n]-\left(F_{fp}[n]-F_{rp}[n]\right)\right\} \\ M_b[n]\ \ddot{y}_b &= R_{fb}[n]+R_{rb}[n]-M_b[n]g \\ I_b\ddot{\theta}_b &= h_{b1}\left(-F_{break}[n]+F_{fp}[n]-F_{rp}[n]\right) \\ &\quad -h_{b2}\left(F_{fud}[n]-F_{rud}[n]\right) \\ &\quad +h_{b3}\left(F_{fld}[n]-F_{rld}[n]\right)+h_{b4}R_{fb}[n]-h_{b5}R_{rb}[n] \end{aligned} \tag{1}$$

where $M_b[n]$ is the mass of the car body, $I_b$ is the moment of inertia of it about the center of gravity, and g is the gravitational acceleration. Let the displacements of (*n*-1)-th, *n*-th, and (*n*+1)-th cars in the forward direction to be $x_b(n\text{-}1)$, $x_b(n)$, and $x_b(n\text{+}1)$, respectively. Then the following equations are satisfied.

$$\begin{aligned} F_{fp}[n] &= k_{ac}\left(x_b(n-1)-x_b(n)\right) \\ F_{rp}[n] &= k_{ac}\left(x_b(n)-x_b(n+1)\right) \\ F_{fud}[n] &= c_{ud}\left(\dot{x}_b(n-1)-\dot{x}_b(n)\right) \\ F_{fld}[n] &= c_{ld}\left(\dot{x}_b(n-1)-\dot{x}_b(n)\right) \\ F_{rud}[n] &= c_{ud}\left(\dot{x}_b(n)-\dot{x}_b(n+1)\right) \\ F_{rld}[n] &= c_{ld}\left(\dot{x}_b(n)-\dot{x}_b(n+1)\right) \end{aligned} \tag{2}$$

Figure 6 shows a simplified bogie model and free-body diagram of the bogie frame. In Fig. 6, $k_{ac}$ is the spring constant of the articulation cone, $k_a$ is the spring constant of the air spring, and $c_{cc}$ is the

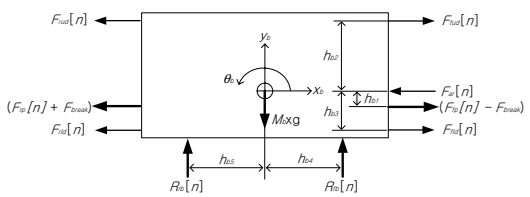


Fig. 5. Free body diagram of *n*-th car body.

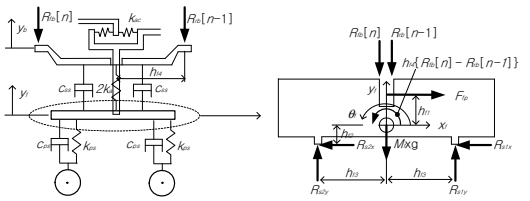


Fig. 6. Bogie model and free-body diagram of the bogie frame.

damping coefficient of the damper which is part of the secondary suspension system.

In the figure, $F_{fp}$, the force by the center pivot inserted into the center of the bogie, denotes the reaction force against the brake force imposed on the car body. As the pivot allows a certain amount of angular motion, it exerts very little moment. $R_{s1x}$, $R_{s1y}$, $R_{s2x}$ and $R_{s2y}$ are the forces acting on the bogie frame by the wheel axles in x and y directions. $y_f$ is the displacement of the bogie frame from the static equilibrium position, and $\theta_f$ is the angle of the bogie frame turning around at the center of gravity in the x-y plane.

When $M_f$ denotes the mass of the bogie frame, $I_f$ denotes the moment of inertia of the bogie frame about center of gravity and $g$ denotes the gravitational acceleration, the equations of motion for the front bogie of the $n$-th car are as follows.

$$\begin{aligned}
&\left(M_f + R_{fb}[n]/g + R_{rb}[n-1]/g\right)\ddot{x}_f = F_{fp} - \left(R_{s1x} + R_{s2x}\right)\\
&\left(M_f + R_{fb}[n]/g + R_{rb}[n-1]/g\right)\ddot{y}_f = \left(R_{s1y} + R_{s2y}\right)\\
&I_f\ddot{\theta}_f = -h_{f1}F_{fp} - h_{f2}\left(R_{s1x} + R_{s2x}\right)\\
&\qquad + h_{f3}\left(R_{s1y} - R_{s2y}\right)\\
&\qquad + h_{f4}\left(R_{fb}[n] - R_{fb}[n-1]\right)
\end{aligned} \tag{3}$$

where

$$\begin{aligned}
R_{s1y} &= -k_{ps}\left(y_f + h_{f3}\theta_f\right) - c_{ps}\left(\dot{y}_f + h_{f3}\dot{\theta}_f\right)\\
R_{s2y} &= -k_{ps}\left(y_f - h_{f3}\theta_f\right) - c_{ps}\left(\dot{y}_f - h_{f3}\dot{\theta}_f\right)
\end{aligned} \tag{4}$$

Since the force acting on the bogie frame by the car body is almost concentrated on the air spring at the center of the bogie, and there is little change in the height of the air spring, the secondary suspension absorbs the impact and transmits the load to the bogie with little displacement caused by the load. Therefore, $R_{fb}[n]$ and $R_{rb}[n\text{-}1]$, the forces that lift up the car body, can be replaced into $M_b[n]/2$ and $M_b[n\text{-}1]/2$, respectively.

As the moment acting on the bogie by the braking torque of the wheel has little influence for the reostatic and eddy-current brake that are mainly used when the train runs at high speed, it is expected that the braking torque would be completely transformed into the force in the opposite direction of train progression, and thus $\theta_f$ is assumed to be very small.

Figure 7 shows the free-body diagram of the wheel, in which, $R_{sx}$ and $R_{sy}$ denote the forces acting by the axles, $N_x$ denotes adhesive force between the wheel and the rail, and $N_y$ denotes vertical reaction force of the rail. And $\tau$ implies braking torque acting on the pair of the wheels installed on the same axis and $\omega$ implies the angular velocity of the wheel.

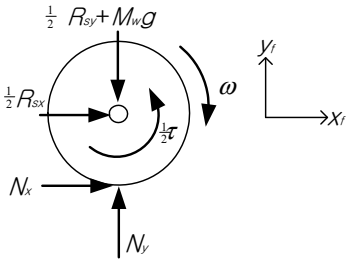


Fig. 7. Free-body diagram of the wheel.

Assuming that the mass of axle is negligible, the wheel may slide on the rail but never detach from the rail, and there exists no relative motion of the bogie frame and the wheel in the forward direction of the train, we may write the equations of motion as follows.

$$\begin{aligned}
&\left(0.5R_{sy}/g + M_w\right)\ddot{x}_f = N_x + 0.5R_{sx}\\
&M_w\ddot{y}_f = 0 = N_y - 0.5R_{sy} - M_w g\\
&I_w\dot{\omega} = -0.5\tau - rN
\end{aligned} \tag{5}$$

where $M_w$ denotes the mass of wheel, $I_w$ the moment of inertia of the wheel with respect to mass center, $r$ the radius of the wheel, and $g$ the gravitational acceleration.

Assuming that the displacement ( $y_b$ - $y_f$) of the air spring and the angle $\theta_f$ of the bogie frame are negligibly small, and there exists no relative motions among the car body, the bogie and the center of mass of the wheel in the direction of train progression, we are able to reduce the number of state variables to represent the dynamics of the train. That is, from the above assumptions, we can define the following state variables for each car.

$$\begin{aligned}
x_1 &= x_b & x_2 &= \dot{x}_b\\
x_3 &= y_b & x_4 &= \dot{y}_b\\
x_5 &= \theta_b & x_6 &= \dot{\theta}_b\\
x_7 &= \omega_{fb} & x_8 &= \omega_{rb}
\end{aligned} \tag{6}$$

The whole state equations for the seven cars using these state variables and dynamic equations obtained in the above can be represented as the following vector form that includes 56 state variables.

$$\dot{\mathbf{x}}_n = \mathbf{f}(\mathbf{x}_{n-1}, \mathbf{x}_n, \mathbf{x}_{n+1}, \tau_n), n = 1,2, \cdots,7 \quad (7)$$

where $\mathbf{x}_n = [\, x_1 , x_2, \cdots, x_8]$ represents the state vector of the $n$-th car, $\tau_n$ represents the braking torque generated by the $n$-th car. We can see that the $n$-th car is affected by both the preceding cars and the following ones.

## 4. HILS for the braking system of KHST

HILS (Hardware-In-the-Loop Simulation) has been in use in Defense and Aerospace industry as early as the 1950s, and then is adopted in automotive industry in the 1990s due to timing and cost involved with the design and verification process of new vehicles (Hanselmann, 1996; Nabi et al., 2004). Since then, several successful HILS have been implemented (Hanselmann, 1997). Earlier applications for HILS are mainly control for the engine and vehicle dynamics, but nowadays all the electronic control units (ECU) in a vehicle series are tested by means of HIL simulation, as the overall network of electronics system in any vehicle has reached an almost unmanageable level of complexity (Lamberg, 2004). For example, it is difficult to test repeatedly the ECU with a real vehicle for all the possible dangerous situations that could occur. In this case, we build a HIL system composed of a real ECU and a DSP board that simulate the vehicle dynamics, and then perform realistic tests for those situations safely and inexpensively.

In this paper, car bodies and bogies are replaced with a DSP board that simulates train dynamics, and braking logic and several phenomena during braking stage are analyzed in real-time. In a viewpoint of braking logic part, it feels as if there is a real train since feedback signals coming into the braking logic part are not different from ones in the real train. Figure 8 shows the schematic diagram of the HIL system constructed in this study. In the figure, the reference input is the speed of the high-speed train, and the output signal is the braking force generated.

In the early stage of the development of KHST, it is impossible to obtain data for the braking system of a real train, and so we built the present system to test breaking logic, to obtain design parameters and to determine design guideline for the braking system, and to predict braking performance of the train. The HIL system includes the DSP board (specifically, DS1102 including TMS 320C31) manufactured by dSPACE GmbH. Real-time programming is accomplished using TI C compiler that supports ANSI C (dSPACE, 2001).

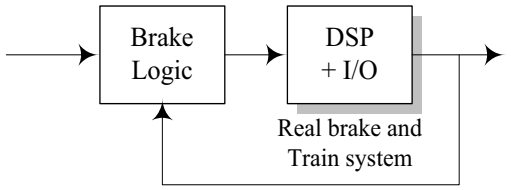


Fig. 8. Schematic diagram of the HIL system for the braking system.

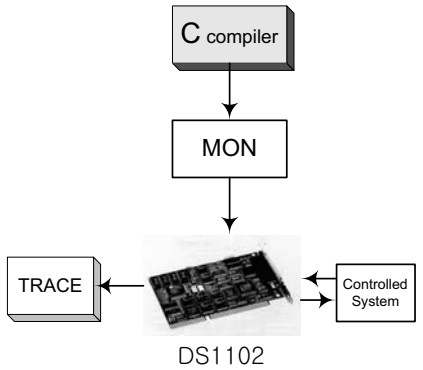


Fig. 9. DSP-CITpro system.

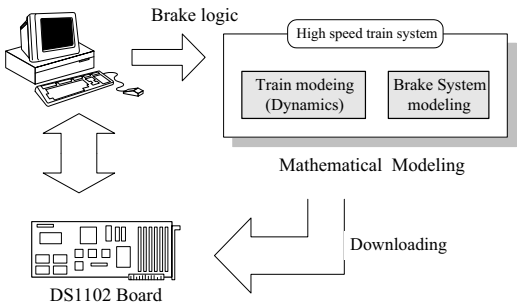


Fig. 10. Architecture for real-time simulations.

Figure 9 shows DSP-CIT tool system. In the figure, TI C compiler generates an object file (MON) that is downloaded into the DSP board. When the downloaded program is executed, TRACE pro-gram enables us to check simulation results in real-time and to store them in PC.

Figure 10 shows the architecture for real-time simulations for the braking system of KHST. Dynamic models of train and brake system are run on DS1102, while brake logic and DSP-CITpro

tool are run on PC. HILS enables us to perform realistic tests repeatedly for the various situations under consistent conditions that could be dangerous in real train tests.

## 5. Braking simulation of KHST

The braking system of KHST has functions of load-dependent control on the passengers' load, velocity-dependent control taking advantage of maximum adhesive force corresponding to each speed, and brake blending to distribute the optimized braking forces to each brake device of the cars.

During the application of brake control, the electric brake units generally apply at high speed at first thing while the air brake units are in charge of the rest of the braking force that the electric brake units cannot undertake. At lower speeds when a smaller brake force is needed, the air brake units come into effect.

In this study on the velocity-dependent control of the train, we settled on the operation ranking of brake systems from high speed to lower speed; regenerative braking (→rheostatic braking) → eddy-current braking → disk braking → wheel disk braking → tread braking.

The brake system can be preferentially adopted according to different operation conditions, but we did not make use of reostatic braking in the simulation under the assumption of normal operation in which regenerative and eddy-current braking are used.

We set the total brake force on the train not to exceed marginal (or maximum) adhesive force for a certain speed, and the marginal adhesive force not to go beyond 450 kN. We employed the profile of adhesion coefficient for each speed to evaluate marginal adhesive force and used the calculation formula for each brake unit from the references (Yujin, 2002).

Since the brake system does not have integrators and dominant closed-loop poles, unit-step response curve of it forms an S-shaped curve, and can be represented using delay time and time constant. If we denote the delay time as $L$, and time constant as $T_c$, and then approximate it as a first-order delay system, the transfer function of it can be represented as follows.

$$G(s) = \frac{Ke^{-Ls}}{T_c s + 1} \tag{8}$$

Let $\mathbf{u}_t(v)$ be input values of braking forces and $\mathbf{F}(t)$ be output values of braking forces for each braking units at speed $v$ and at a tentative time $t$ after brake command takes effect. Then from the above transfer function, the output equation can be described as follows, where a ready-time of each unit is also considered.

$$\mathbf{F}(t) = \begin{cases} \mathbf{K}\mathbf{u}_{(t-L-ready\ time)}(v) - \mathbf{T}_c \dot{\mathbf{F}}(t) & t \geq L + ready\ time \\ 0 & t < L + ready\ time \end{cases} \tag{9}$$

where $\mathbf{u}_t(v)$ = [ $F_{rege}(v)$, $F_{rheo}(v)$, $F_{eddy}(v)$, $F_{disk}(v)$, $F_{wheel}(v)$ , $F_{tread}(v)$ ] is a vector, $\mathbf{F}(t)$, $\mathbf{K}$, and $\mathbf{T}_c$ are also vector quantities.

Within the HILS of KHST's brake system, the brake blending logic distributes braking forces at each brake unit appropriately according to the speed of the train, and real-time simulations are put into practice using brake models representing dynamic characteristics and other conditions. Figure 11 illustrates the entire block diagram for the braking system of KHST.

In Fig. 11, Brake blending control unit (BBCU) blends braking forces for each brake unit and send blended brake forces to each brake unit. Traction control unit (TCU) undertakes the control of regenerative (or rheostatic) brake force depending on brake force commands coming from BBCU. Eddy-current control unit (EECU) controls eddy-current brake force according to the values from BBCU, and brake control unit (BCU) conducts air brake control according to varying command values of the air brake from BBCU.

Since Eq. (8) calculates brake forces in continuous-time domain, it is inconvenient for Eq. (8) to be immediately employed in the program for the real-time simulation. Therefore, the discrete-time equation corresponding to Eq. (8) is obtained as follows by conducting z-transformation of Eq. (8) and using zero–order hold.

$$y(k+2) = p \cdot y(k+1) + a_1 \cdot u(k+1) + a_2 \cdot u(k) \tag{10}$$

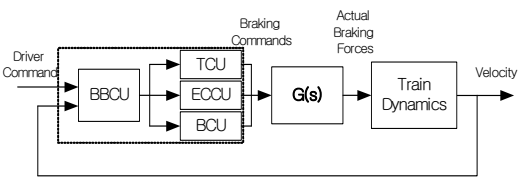


Fig. 11. Block diagram of the braking system.

where $u(k)$ is an input and $y(k)$ is an output. For the derivation of parameters and the specific values for each brake unit, refer to the paper (Lee et al., 2002).

## 6. Simulation results

In this section, we describe the results of real-time simulations on seven cars of KHST in the HIL system using the dSPACE board. The real-time simulation takes dynamic characteristics of cars and interaction between cars into consideration. We performed the simulation test on braking performance under the assumption that each brake unit controller and electricity lines for regenerative brake are normal.

Figure 12 depicts adhesive force limit (that is, adhesion coefficient) and maximum braking force for each brake unit corresponding to train velocity. Figure 13 shows braking force commands with respect to time for each brake unit that are distributed from BBCU when total braking force is constrained to 450 kN.

Figure 14 shows actual brake forces of the seven cars (the results of simulation) that were brought on by brake command on the straight horizontal rail section. Figure 15 illustrates the outcome of the disc brake unit among various brake units with a view to comparing the brake force command values with the actual brake forces. In those results of the real-time simulation of the HIL system, we see that the actual brake forces are delayed by ready-time, delay time, and time constant, as expected.

The simulation results of the HIL system in Fig. 16 shows that it takes the train at a speed of 350 km/h 98.4 seconds to come to a complete stop, and the braking distance is 4774 m, which satisfies the 4800m requirement of the KHST specification.

Figure 17 depicts the actual deceleration profile during braking time, which shows that the maximum declaration exists within the comfort limit for passengers of 1.4725 m/s$^2$.

To catch a grasp of each car's dynamic characteristics, we consider the 4$^{th}$ car located in the middle of the train. Figures 18, 19 and 20 demonstrate the results of the simulations for the fourth car. Figure 18 shows the car body's pitch angle with respect to the mass center. We see that the pitch rotation is within the limit of 0.0036 rad. Figure 19 shows that the dynamic load on the front axle exists between 95 and 140 kN.

Figure 20 shows the forces acting on the connecting damper with the third car and the fourth car in the lower part of the car body. In the figure, the instant when the force reaches zero means there is no relative motion between cars, and a maximum of 8.8 kN force is in effect. This value comes from the relative velocity limit between two cars that we set according to the given data.

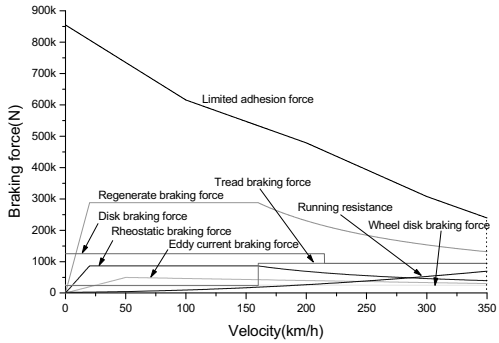


Fig. 12. Adhesive force limit and maximum braking force diagram for each brake unit.

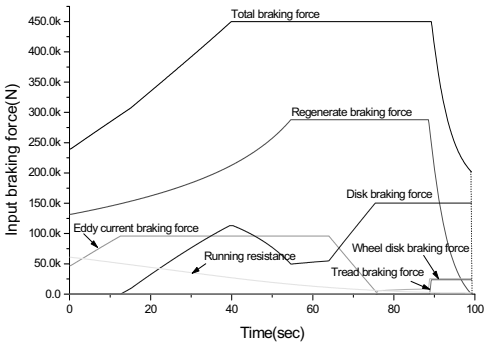


Fig. 13. Each brake force command distributed from BBCU.

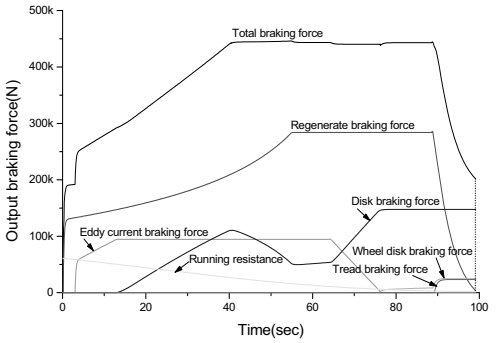


Fig. 14. Actual brake force of each brake unit. (Simulation result).

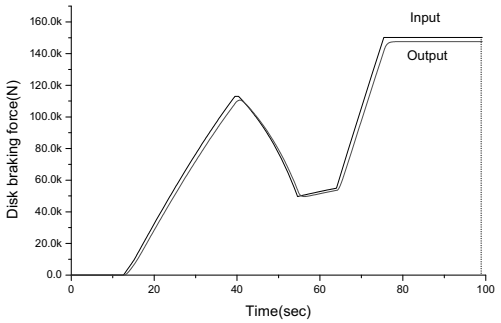


Fig. 15. Disk brake force command and actual brake force. (Simulation result)

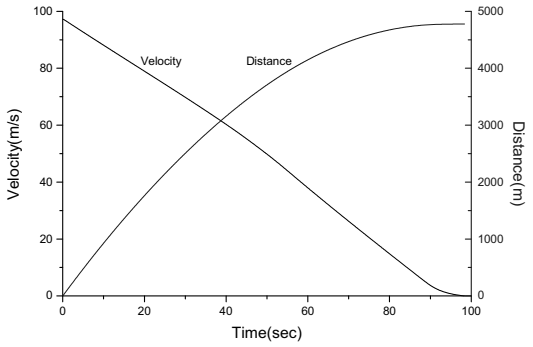


Fig. 16. Braking distance and velocity. (Simulation result)

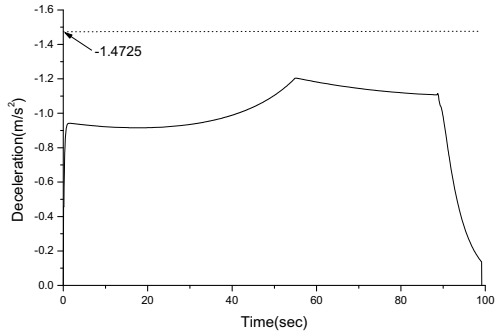


Fig. 17. Deceleration profile. (Simulation result)

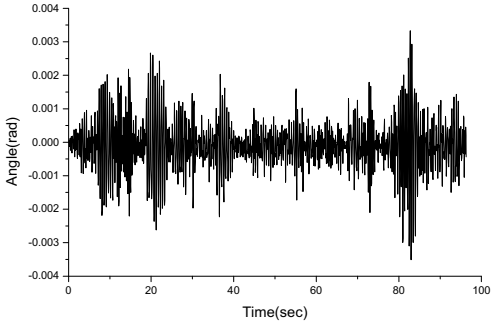


Fig. 18. Pitch angle of the 4th car with respect to the center of gravity. (Simulation result)

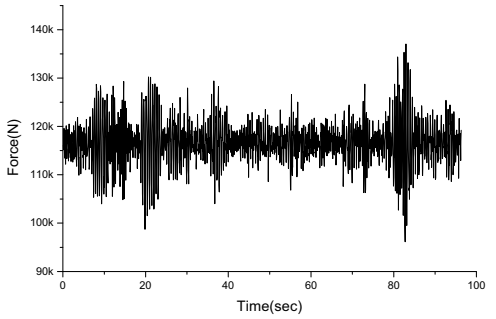


Fig. 19. Force acting on the front axle of the 4th car. (Simulation result)

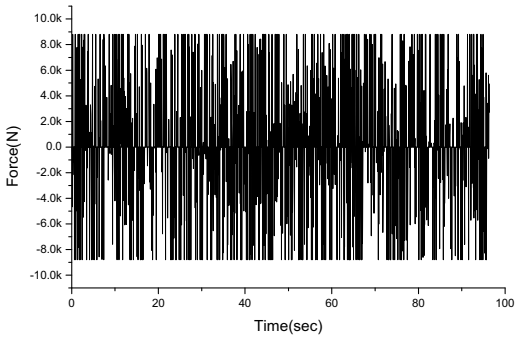


Fig. 20. Force acting on the lower damper between the 3rd and 4th car. (Simulation result)

## 7. Conclusion

This study has attempted to predict different possibilities when the braking system using the DSP board manufactured by dSPACE is put on the Korean High-Speed Train that is composed of 7 cars. To obtain the realistic simulation results similar to the actual brake operation, we built the HIL system after modeling each characteristic of the seven cars and the connecting devices into a dynamic equation. Then we applied the predicted parameters and the specifications of the prototype cars, and conducted real-time simulations. We drew some conclusions on the braking system of the Korean High-Speed Train as follows.

- If all of the brake units are normally operating, the braking distance satisfies the requirement of the specification even though the marginal brake force is restricted within 450 kN.
- As the sum total of the instantaneous brake force is constant, the air brake force increased in the lower speed section.
- Deceleration does not exceed the comfort limit for passengers of 1.4725 m/s$^2$.

• Within the bounds of keeping the characteristics of the actual devices undistorted, devising how to distribute the brake force is effective in predicting the actual brake force.

The follow-up research may have to obtain the actual design parameters of KHST after it is manufactured, and revise the HIL system to be more realistic by comparing the simulation result and actual experimental results of KHST.

## Acknowledgement

The author gratefully acknowledges the partial financial support from the Seoul R&BD Support Program (e-Printing Cluster Project 2-C) for this research. Also, he thanks Mr. Jae-Boong Jung, Nam-Jin Lee, and Won-Ju Hwang for their helps.

## References

Chung, K. R., 1998, "Development of Conceptual Design and Evaluation Method for the High-Speed Train," *The 2nd Year Report of the G7 KHST project*, pp. 59~86 (In Korean).

dSPACE GmbH, 2001, *dSPACE User' Guide*.

Hanselmann, H., 1996, "Hardware-In-the-Loop Simulation Testing and its Integration into a CACSD Toolset," *IEEE International Symposium on Computer-Aided Control System Design*.

Hanselmann, H., 1997, "Advances in Desktop Hardware-In-the-Loop Simulation," *SAE Technical Paper 970932.*

Hur, N., Kim, S. R., Kim, W. and Lee, S., 2004, "Wind Pressure Transients in the Tunnel inside a Station Caused by a Passing High Speed Train," *KSME International Journal*, Vol. 18, No. 9, pp. 1614~1622.

Hwang, W. J., Kang, C. G., 2001, "HILS of the Braking System of a High Speed Train," *J of Control, Automation and Systems Engineering,* Vol. 7, No. 5, pp. 432~437 (In Korean).

Kato, I., Terumichi, Y., Adachi, M. and Sogabe, K., 2005, "Dynamics of Track/Wheel Systems on High-Speed Vehicles," *Journal of Mechanical Science and Technology*, Vol. 19, No. 1, pp. 328~335.

Korea Railroad Research Institute, 2002, "Development of the Korean High-Speed Train," *Report of G7 KHST project* (In Korean).

Lamberg, K., 2004, "Systematic Testing – Modern Solutions for Hardware-In-the-Loop-Simulation," dSPACE website www.dspace.de/ww/en/pub/company/medien/papers.htm (also Automotive Electronics 09/2002).

Lee, N. J. and Kang, C. G., 2002, "Brake Force Simulation of a High Speed Train Using a Dynamic Model," *J of Control, Automation and Systems Engineering*, Vol. 8, No. 1, pp. 46~53 (In Korean).

Matsumoto, K., Suda, Y., Komine, H., Nakai, T., Tomeoka, M., Shimizu, K., Tanimoto, M., Kishimoto, Y. and Fujii, T., 2005, "A Proposal of Wheel/Rail Contact Model for Friction Control," *Journal of Mechanical Science and Technology*, Vol. 19, No. 1, pp. 437~443.

Miyachi, M., Matsumoto, K. and Matsuki, T., 1996, "The New Generation of ATC System for Super High-speed Operation on Shinkansen Lines," *Proc of IEEE 46th Vehicular Technology Conference* Vol. 3, pp. 1613~1617.

Nabi, S., Balike, M., Allen, J. and Rzemien, K., 2004, "An Overview of Hardware-In-the-Loop Testing Systems at Visteon," *SAE Technical Paper 2004-01-1240*, SAE World Congress, Detroit, Michigan.

Rahn, T., 1986, "The German Federal Railway high-speed train," *Technica*, Vol. 35, No. 23, pp. 47~51.

Schiehlen, W., 2005, "Recent Developments in Multibody Dynamics," *Journal of Mechanical Science and Technology*, Vol. 19, No. 1, pp. 227~236.

Yujin Machinery, Ltd., 2002, "Development of the brake system of KHST," *The Report of the KHST project*(In Korean).